

Oxygen vacancy estimation of high k metal gate using thermal dynamic model

H. L. Chang and M. S. Liang

Citation: *Applied Physics Letters* **97**, 041912 (2010); doi: 10.1063/1.3473772

View online: <http://dx.doi.org/10.1063/1.3473772>

View Table of Contents: <http://scitation.aip.org/content/aip/journal/apl/97/4?ver=pdfcov>

Published by the *AIP Publishing*

Articles you may be interested in

Fluorine implantation for effective work function control in p-type metal-oxide-semiconductor high- k metal gate stacks

J. Vac. Sci. Technol. B **29**, 01A905 (2011); 10.1116/1.3521471

Electron and hole components of tunneling currents through an interfacial oxide-high- k gate stack in metal-oxide-semiconductor capacitors

J. Appl. Phys. **108**, 093711 (2010); 10.1063/1.3503457

Oxygen passivation of vacancy defects in metal-nitride gated HfO₂ / SiO₂ / Si devices

Appl. Phys. Lett. **95**, 042901 (2009); 10.1063/1.3186075

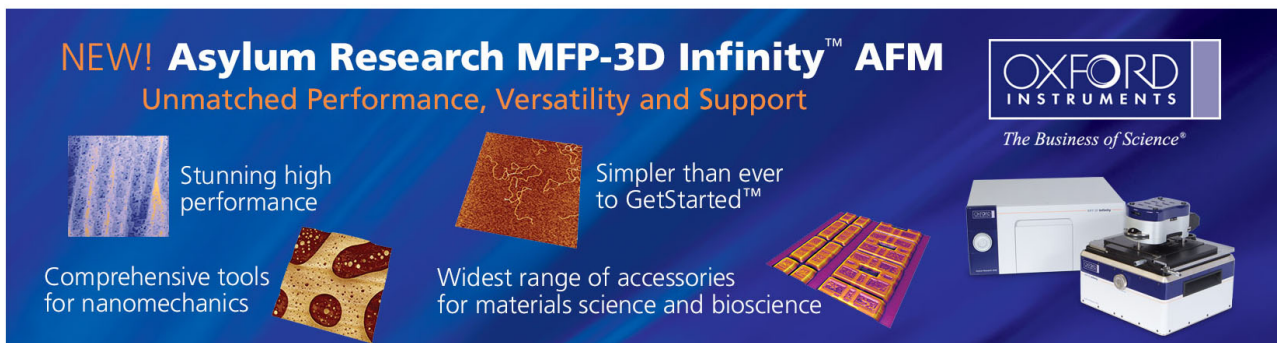
Evaluation of titanium silicon nitride as gate electrodes for complementary metal-oxide semiconductor

Appl. Phys. Lett. **88**, 142113 (2006); 10.1063/1.2188380

Engineering chemically abrupt high- k metal oxidesilicon interfaces using an oxygen-gettering metal overlayer

J. Appl. Phys. **96**, 3467 (2004); 10.1063/1.1776636

NEW! Asylum Research MFP-3D Infinity™ AFM
Unmatched Performance, Versatility and Support



OXFORD INSTRUMENTS
The Business of Science®

Stunning high performance

Simpler than ever to GetStarted™

Comprehensive tools for nanomechanics

Widest range of accessories for materials science and bioscience

Oxygen vacancy estimation of high k metal gate using thermal dynamic model

H. L. Chang^{a)} and M. S. Liang

Department of Material Science and Engineering, National Chiao Tung University,
1001 University Road, Hsinchu, Taiwan 300, People's Republic of China

(Received 11 February 2010; accepted 7 July 2010; published online 30 July 2010)

Oxygen vacancies are electronic defects in materials. In a metal oxide system, the distribution of such vacancies is determined by the oxygen affinity. This study predicts the oxygen vacancy concentration in a high-k/metal gate system using a developed thermal dynamic model. A system with Ti:N=2 has a 200 mV lower flat band voltage than an N rich metal. The Gibbs free energy of formation of oxygen vacancies, ~ 0.5 eV, is derived from flat band voltage shifts and created neutral oxygen vacancy. The oxygen vacancy model based on estimating thermal dynamics is proposed. © 2010 American Institute of Physics. [doi:10.1063/1.3473772]

The aggressive scaling down of complementary metal oxide semiconductor (CMOS) transistors depends on the use of metal oxides with high dielectric constants to overcome the physical limitations of SiO₂ interfacial layers. To date, Hf-based metal oxides such as HfO₂, Hf silicate, and HfSiON are of the great interest attracting the most attention. The effective work function (EWF) must be adjusted to meet the reliability criteria by engineering the high-k/metal gate stack.¹ Various study have addressed the tuning of the EWF by incorporation of interface dipole layers that are formed separately by generating a lanthanide-based and Al-based n- and p-metal-oxide-semiconductor field-effect transistors (MOSFETs), respectively.² Etching dielectric metal oxide is difficult. Engineering the metal gate materials can be effective in changing the EWF. The tunable and midgap TiN with a work function of 4.3–4.5 eV, adjusted by varying the Ti to N ratio, is the most promising candidates. The use of a high-k/metal gate stack raises numerous challenging: the n and p type planer bulk CMOS devices must have near Si band edge work functions (4.05 eV and 5.15 eV for NMOS and PMOS, respectively). Recently, oxygen vacancies have been proposed to be responsible for the threshold voltage (V_{th}) shifts. The present authors have proposed that oxygen vacancy (V_o) induced interface dipoles may be responsible for the large flat band voltage (V_{fb}) shifts. Fermi level pinning explains the effect of oxygen vacancies on the substantial threshold voltage shifts in a p+poly Si gate.^{3,4}

This work introduces the use of a metal gate TiN to adjust EWF by changing the Ti/N ratio. An SiO₂ film was deposited at 10 Å using a chemical oxidation process and SC1 solution. HfO₂ was at 15 Å in a atomic layer deposition process using precursor [(MeCp)₂Hf Me(mmp), mmp = OCMe₂CH₂OMe] on an OH⁻ treated surface. TiN was prepared at 50 Å by rf PVD by adjusting the Ti to N ratio. Three films A, B, and C, with TiN/HfO₂/SiO₂ gate stacks were used: scheme A had Ti/N=2, scheme B had Ti/N=1.5, and scheme C had Ti/N=1. Capacitance-voltage (CV) measurements were made in parallel mode (at 100 kHz) to determine the dependence of the V_{fb} .

The flat band voltage in TiN/HfO₂/SiO₂/Si capacitors was investigated as function of the metal composition. The

flat band voltage shifted in the negative direction as the Ti to N ratio increased. For a Ti to N ratio of 2:1.5:1, the band voltages were -415, -350, and -215 mV. The flat band shifts increase with Ti concentration, indicating that the interface dipoles contribute to V_{fb} . Figure 1 shows the C-V curves of schemes A, B, and C.

To elucidate the physical behavior of high-k metal/gate stacks, x-ray photoelectron spectrometer (XPS) and transmission electron microscopy (TEM) are used to determine the bonding structure and microstructures. Figure 2 shows the evolution of SiO₂ and HfO₂ with temperature as determined by XPS analysis. No SiO₂ is present upon Ti/N = 2:1 deposition but the SiO₂ is observed again after rapid thermal annealing at 1273 K. TEM is applied to confirm the XPS analysis. However, HfO₂/SiO₂ thickness changes are negligible at Ti/N=1. Figures 3(a) and 3(b) present the deposition of TiN 50 Å/HfO₂ 15 Å/SiO₂ 10 Å for scheme A, at room temperature and after rapid thermal processing, respectively. The SiO₂ layer is absent and an increase in the thickness of HfO₂ by 25 Å is observed. To understand the redistribution of oxygen, the standard free energy change is expressed in terms of the standard enthalpy and entropy of the reaction, using $\Delta G^\circ = \Delta H^\circ - T\Delta S^\circ$. Analytical methods introduced for M-X (M=Ti, Hf, and Si, X=O) have been applied to study oxygen affinity of the metals.⁵ Thus a plot of ΔG° against temperature can be used to compare the oxidation and dissociation behaviors when the reactions are considered in terms of the consumption of one mole of oxygen.⁶ Figure 4 plots the Gibbs free energy

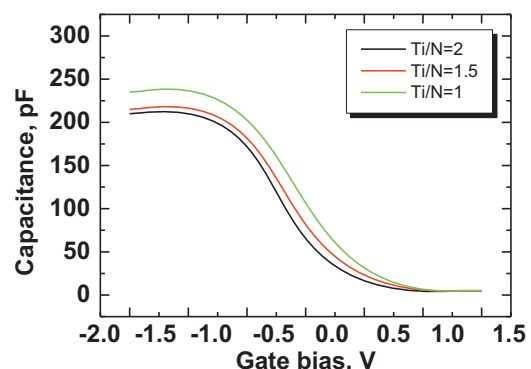


FIG. 1. (Color) Systematic variation in flatband voltage in HfO₂/TiN capacitors with different Ti to N ratios.

^{a)}Electronic mail: gladies.chang@gmail.com.

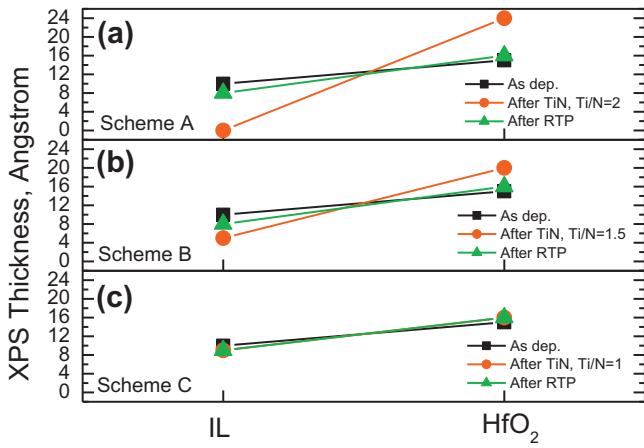


FIG. 2. (Color) IL/HfO₂ thickness evolution (a) scheme A, (b) scheme B, and (c) scheme C.

for the SiO₂, HfO₂, Ti₂O, TiO, Ti₂O₃, Ti₃O₅, TiO₂, and TiN as a function of temperature. The standard Gibbs free energy change for the formation of metal oxide as a function of temperature can be expressed by the following equations:

$$2\text{Ti} + \frac{1}{2}\text{O}_2 = \text{Ti}_2\text{O}, \quad \Delta G^\circ = -279\,400 + 43.5 T, \quad \text{cal/mole}, \quad (1)$$

$$2\text{Ti} + \text{O}_2 = 2\text{TiO}, \quad \Delta G^\circ = -244\,600 + 42.6 T, \quad \text{cal/mole}, \quad (2)$$

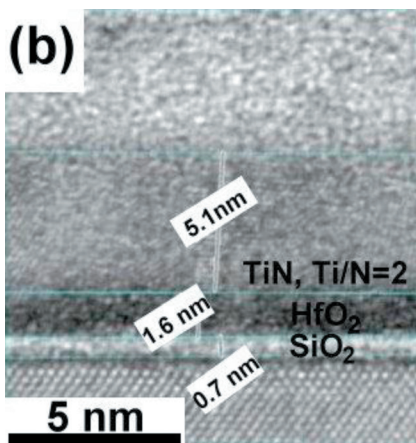
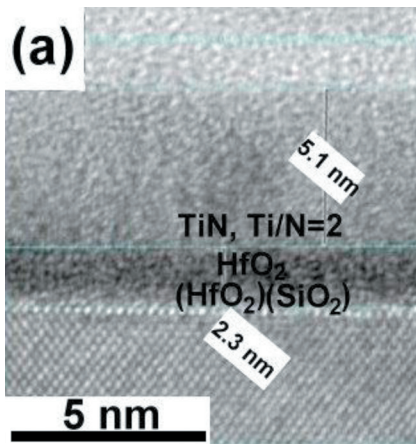


FIG. 3. (Color) TEM image of scheme A (a) at 298 K and (b) at 1273 K.

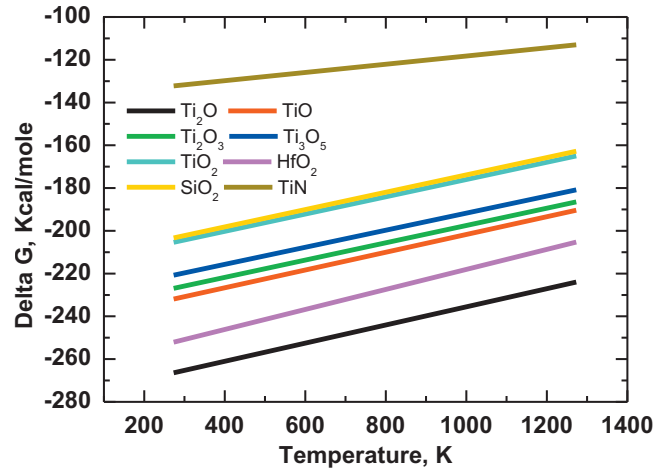


FIG. 4. (Color) Gibbs free energy vs temperature for the SiO₂, HfO₂, Ti₂O, TiO, Ti₂O₃, Ti₃O₅, TiO₂, and TiN.

$$\frac{4}{3}\text{Ti} + \text{O}_2 = \frac{2}{3}\text{Ti}_2\text{O}_3, \quad \Delta G^\circ = -239\,166 + 41.2 T, \quad \text{cal/mole}, \quad (3)$$

$$\frac{6}{5}\text{Ti} + \text{O}_2 = \frac{2}{5}\text{Ti}_3\text{O}_5, \quad \Delta G^\circ = -232\,950 + 40.9 T, \quad \text{cal/mole}, \quad (4)$$

$$\text{Ti} + \text{O}_2 = \text{TiO}_2, \quad \Delta G^\circ = -217\,703 + 41.4 T, \quad \text{cal/mole}, \quad (5)$$

$$2\text{Ti} + \text{O}_2 = 2\text{TiO}, \quad \Delta G^\circ = -244\,600 + 42.6 T, \quad \text{cal/mole}, \quad (6)$$

$$\text{Hf} + \text{O}_2 = \text{HfO}_2, \quad \Delta G^\circ = -266\,435 + 48.1 T, \quad \text{cal/mole}, \quad (7)$$

$$\text{Si} + \text{O}_2 = \text{SiO}_2, \quad \Delta G^\circ = -215\,600 + 41.5 T, \quad \text{cal/mole}. \quad (8)$$

Figure 5 shows the Si, Hf, and Ti predominance phase diagram as the function of oxygen and nitrogen partial pressure at a temperature of 1273 K. The equilibrium of O₂ or N₂ pressure can be derived from the standard Gibbs free energy changed associated with M-O or M-N system, where ΔG° is Gibbs free energy change, R is the gas constant, and T is the absolute temperature.⁷

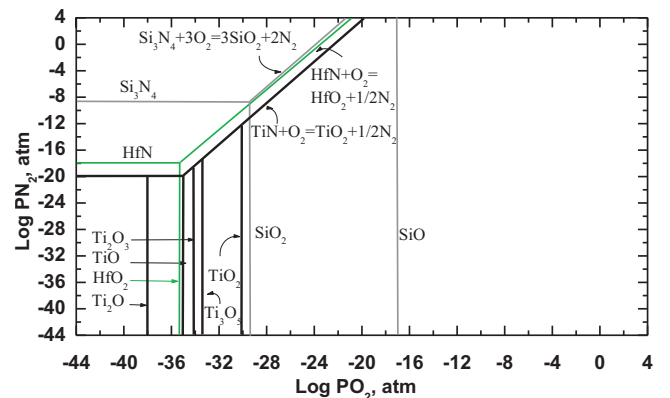
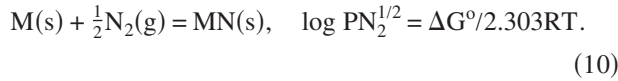
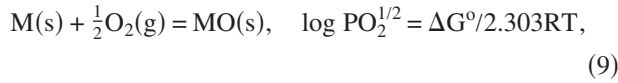


FIG. 5. (Color) Si-Hf-Ti predominance phase diagram, temperature = 1273 K.



The partial pressure of oxygen in a system is commonly referred to as its oxygen potential $\mu_{O_2} = \mu_{O_2}^0 + RT \ln PO_2$. The value of oxygen affinities in the oxidation reaction, Ti in a system with an oxygen potential of a chamber 10^{-10} atm at 298 and 1273 K can be evaluated from Fig. 5.

Hence, in such an atmosphere, Ti in this system undergoes spontaneous oxidation. The oxygen affinities follow the order $Ti_2O > HfO_2 > TiO_2 > SiO_2 > TiN$. The incorporation of oxygen from the HfO_2 into the Ti rich metal is energetically favorable. Supplementing the oxygen in HfO_2 from SiO_2 underlayer is also energetically favorable, since HfO_2 has a higher oxygen affinity than SiO_2 . When the metal gate of TiN films with different Ti to N ratios, the first phase that is formed by the oxidation of TiN is Ti_2O . Consider the incorporation of oxygen into the Ti-rich electrode; the energy is gained by the formation of Ti_2O , the metal electrode acts as drains of oxygen by dissolving it, yielding oxygen deficient HfO_2 and the absence of an SiO_2 layer. The SiO_2 has a lower oxygen affinity in the Ti/ HfO_2 system. In the Ti-rich TiN electrode, transfer of oxygen and the absence of interfacial SiO_2 at low temperature involves the following mechanism; (1) the transportation of oxygen atoms from HfO_2 sites to TiN (Ti-rich electrode), and the dissociation of oxygen in the electrode: $2Hf_{Hf}^x + O_O^x = 2Hf'_{Hf} + V_O^- + \frac{1}{2}O_2$; (2) the transportation of oxygen atoms from SiO_2 sites to HfO_2 sites: $V_O^- + 2e' + \frac{1}{2}O_2 = O_{Hf}$; the oxygen deficiency of interfacial layer causes the transitional silicate formation (3) the reaction between silicate and HfO_2 : the mixing of $SiO_{x,x<2}$ and HfO_2 is energy gain at room temperature from the $SiO_{x,x<2} + HfO_2 = (HfO_2)(SiO_{x,x<2})$,⁸ The major contribution of silicate to the HfO_2 causes an increase in HfO_2 thickness. (4) In high temperature annealing, the spinodal decomposition of the metastable $HfSiO_4$ phase can cause phase separation of HfO_2 and SiO_2 .⁹ Therefore, the SiO_2 and HfO_2 layers have physical thicknesses that are similar to their as-deposited thickness. However, for the Ti:N=1 electrode, the oxygen transportation and interaction proceed as follows: (1) incorporation of oxygen from the ambient into the metal gate, $\frac{1}{2}O_{2(g)} = O'_M$, (2) slight reaction of silicate and HfO_2 to form a solid solution $(HfO_2)(SiO_x)$ at below T_g , because the degree of SiO_2 oxygen deficiency is negligible, and (3) slight spinodal decomposition of $(HfO_2)(SiO_x)$ into its original forms.

When one more of Ti_2O is formed, the concentration of oxygen sites 10^{21} cm^{-3} is equivalent to the concentration of requested oxygen atoms in the system, implying that the amount of oxygen vacancies is formed.

According to flat band voltage shifts and fixed charge at the high k insulators giving

$$\Delta V_{fb} = \frac{1}{C_{eff}(t_1 + t_2)} \int_0^{t_1} x \rho_{HK}(x) dx, \quad (11)$$

t_1 and t_2 are high k and oxide thickness and ρ_{HK} is the high k charge density,

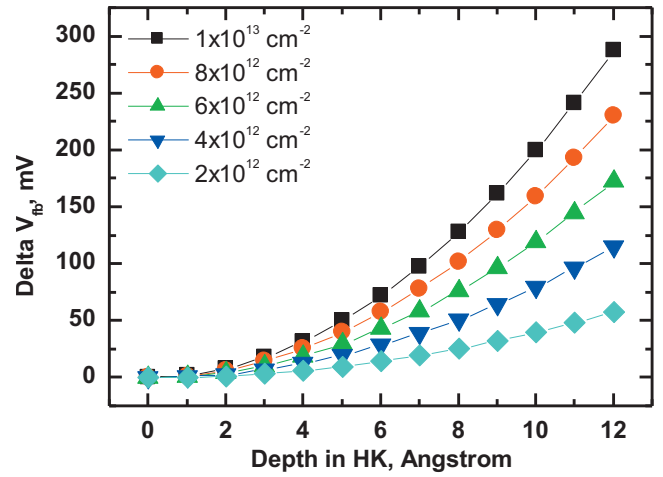


FIG. 6. (Color) Estimated flat band voltage shift vs oxygen vacancy concentration in high k film.

Figure 6 shows a shift in V_{fb} of 100 mV associated with 10^{12} cm^{-3} oxygen vacancies. A neutral vacancy can be created in HfO_2 with two electrons in its vacancy level. These electrons gain energy by falling into the metal Fermi energy E_f . The number of effective charged vacancies is expressed by $n = n_0 \exp(-\Delta G/kT)$, where n_0 is the oxygen ion density in HfO_2 , $n_0 = 6.2 \times 10^{21} \text{ cm}^{-3}$. ΔG is estimated to be 0.5 eV, which value is consistent to the predicted formation energy ~ 0.7 eV, indicating that enough vacancies are created to pin E_f . According, when a Ti-rich electrode is used, oxygen vacancies contribute to the negative shift in V_{fb} .

V_{fb} is tuned as a function to oxygen affinity by applying a metal electrode herein in this work. The required Gibbs free energy for V_{fb} shifts is estimated by evaluating the number of oxygen vacancies in physical and electrical performances. The association between oxygen transportation and vacancy formation is explained by thermal dynamic estimation. The fact that oxygen transportation is responsible for the interaction of TiN/ HfO_2 / SiO_2 /Si systems at room temperature demonstrates the importance of controllable integration.

The authors would like to thank National Science Council of the Republic of China, Taiwan for financially supporting this research.

¹S. B. Samavedam, L. B. La, J. S. Smith, S. Dakshina-Murthy, E. Luckowski, J. Schaeffer, M. Zavala, R. Martin, V. Dhandapani, D. Triyoso, H. H. Tseng, P. J. Tobin, D. C. Gilmer, C. Hobbs, W. J. Taylor, J. M. Grant, R. J. Hegade, J. Mogab, C. Thomas, P. Abramavitz, M. Moosa, J. Conner, J. Jiang, V. Arunachalam, M. Sadd, B.-Y. Ngvyen, and B. White, Tech. Dig. - Int. Electron Devices Meet. **2002**, 2002.

²H. N. Alshareef, H. C. Wen, P. Kirsch, P. Majihi, B. H. Lee, and R. Jammy, *Appl. Phys. Lett.* **89**, 232103 (2006).

³S. Guha and V. Narayanan, *Phys. Rev. Lett.* **98**, 196101 (2007).

⁴K. Shiraishi, K. Yamada, K. Torii, Y. Akasaka, K. Nakajima, M. Konno, T. Chikyow, H. Kitajima, and T. Arikado, *Jpn. J. Appl. Phys., Part 2* **43**, L1413 (2004).

⁵G. V. Samsonov and I. M. Vinitiski, *Handbook of Refractory Compounds* (FI/Plenum, New York, 1980).

⁶R. T. Dehoff, *Thermodynamics in Material Science* (McGraw-Hill, Singapore, 1993), p. 330.

⁷R. T. Dehoff, *Thermodynamics in Material Science* (McGraw-Hill, Singapore, 1993), p. 132.

⁸A. A. Demkov and A. Navrotsky, *Materials fundamentals of Gate Dielectrics* (Springer, New York, 2005), p. 71.

⁹J. Robertson, *Eur. Phys. J.: Appl. Phys.* **28**, 265 (2004).